Generalised fracture mechanics approach to the interfacial failure analysis of a bonded steel-concrete joint

Wouter De Corte, Peter Helincks, Veerle Boel
Research Group Schoonmeersen, Department of Structural Engineering, Faculty of Engineering and Architecture, Ghent University Valentin Vaerwyckweg 1, B-9000, Ghent, Belgium.
Wouter.DeCorte@UGent.be, Peter.Helincks@UGent.be, Veerle.Boel@UGent.be

Jan Klusák
CEITEC IPM, Institute of Physics of Materials, Academy of Sciences of the Czech Republic, Žižkova 22, Brno 616 62, Czech Republic.
klusak@ipm.cz

Stanislav Seitl
Institute of Physics of Materials, Academy of Sciences of the Czech Republic, Žižkova 22, 616 62 Brno, Czech Republic.
seitl@ipm.cz

Geert De Schutter
Magnel Laboratory for Concrete Research, Department of Structural Engineering, Faculty of Engineering and Architecture, Ghent University, Technologiepark-Zwijnaarde 904, B-9052, Ghent, Belgium.
Geert.Deschutter@ugent.be

ABSTRACT. Steel-concrete joints are often made by welded shear studs. However, this connection reduces the fatigue strength, especially in situations where locally concentrated loads occur with a large number of load cycles e.g. in bridge decks. In this paper the shear bond strength between steel and ultra-high performance concrete (UHPC) without welded mechanical shear connectors is evaluated through push-out tests and a generalized fracture mechanics approach based on analytical and finite element analyses. The connection is achieved by an epoxy adhesive layer gritted with granules. In the tests, specimens made with various manners of preparation of the epoxy interlayer are tested experimentally. Numerical-analytical 2D and 3D modelling of a steel-concrete connection is performed without and with the epoxy interlayer. The model of a bi-material notch with various geometrical and material properties is used to simulate various singular stress concentrators that can be responsible for failure initiation. Thus conditions of crack initiation can be predicted from knowledge of the standard mechanical and fracture-mechanics properties of particular materials. Results of the fracture-mechanics studies are compared with each other and with

Citation: De Corte, W., Klusák, J., Helincks, P., Seitl, S., Boel, V., De Schutter, G., Generalised fracture mechanics approach to the failure analysis of a bonded steel-concrete joint, Frattura ed Integrità Strutturale, 42 (2017) 147-160.

Received: 16.06.2017
Accepted: 21.06.2017
Published: 01.10.2017

experimental results. On the basis of the comparison, the 2D simulation of the steel-concrete connection without the epoxy interlayer is shown to be suitable for the estimation of failure conditions.

KEYWORDS. Fracture mechanics; Steel-concrete joint; Epoxy adhesive; Interfacial properties, Push-out test; Numerical study.

INTRODUCTION

Often, concrete and steel are combined in structural elements. The tensile strength of steel and the compressive strength of concrete co-operate, but a good connection between both materials is required to obtain the level of structural performance. Mechanical shear connectors of various types, welded on the steel surface, are often applied to ensure this connection. However, since the 1960's [1] adhesive bonding techniques have been tested by various authors. In this way stress concentrations generated by the stud connectors are avoided and welding is unnecessary. The latter is advantageous in view of fatigue. In recent years, adhesive bonding has become an accepted technique for strengthening reinforced concrete structures with steel plates [2, 3] or more common CFRP (carbon fibre reinforced polymer) plates [4-6]. Additionally, the technique is also valuable for steel-concrete composite beams [7-12]. In order to evaluate the bonding resistance and to study the failure mechanisms, most often push-out tests are performed [10-13]. In this paper the results of such tests, together with the influences of changes to various parameters, will be the base of a generalized fracture mechanics based analysis. Such an analysis is necessary since typical push-out tests may exhibit failure at the steel to concrete, steel to adhesive or adhesive to concrete interfaces. Such critical points can be modelled as bi-material notches. The notches of this kind are general singular stress concentrators. Whereas cracks in components can be assessed by standard fracture mechanics approaches using comparison of the stress intensity factor (SIF) with its critical value (fracture toughness), in case of presence of bi-material interface, approaches of this kind cannot be used. The test specimens are assessed here from the generalized linear elastic fracture mechanics point of view [14-16]. Using analytical-numerical approaches, the test configuration is evaluated in order to estimate the critical applied load corresponding to failure initiation in locations of the stress concentration. In the first part of the paper, the generalised fracture mechanics approach and its application for this problem will be explained, in the second part, the experimental work will be addressed, where in the third part the numerical study will demonstrate the applicability of the method for assessment of the failure of a bonded steel-concrete joint.

FRACTURE MECHANICS APPROACH TO A BI-MATERIAL NOTCH

The stress distribution in the vicinity of a bi-material notch tip is found in the form of the sum of singular terms corresponding to two singularity exponents p_k, where $k = 1, 2$. Therefore, the singular stress components can be expressed in the form (Eq. 1):

$$\sigma_{ij,m} = \sum_{k=1}^{2} \frac{H_k}{\sqrt{2\pi}} r^{-p_k} F_{ijkm} \tag{1}$$

where the subscripts i, j denote the polar coordinates (r, θ) (the origin of the polar coordinate system is in the notch tip) and the subscript $m = 1, 2$ refers to material 1 or 2 (Fig. 1). Expressions H_k for $k = 1, 2$ are the generalized stress intensity factors (GSIF) which result from a numerical solution for given boundary conditions. F_{ijkm} are known functions of polar coordinates, geometry and materials of the notch [16-17]. In order to estimate conditions of failure of specimens with a bi-material notch, generalized stability criteria must be used. Those criteria describe conditions of fracture initiation from the stress concentrator, and do not consider the conditions of consequent crack propagation. Stability criteria are suggested with the help of a controlling magnitude which is well defined in the case of a crack in homogeneous material and in the case of a bi-material notch as well. Moreover the controlling magnitude has the same meaning in both cases (crack and notch). Such a magnitude can be represented by an average value of tangential stress, or an average value of the strain energy density factor, for details see [16].

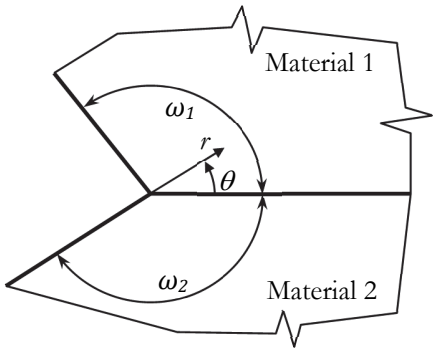

Figure 1: A bi-material notch (with corresponding polar co-ordinate system)

In this paper the modified maximum tangential stress (MTS) criterion [18] is used. The average value of the tangential stress is evaluated over a certain distance d:

$$\overline{\sigma_{\theta\theta,m}}(\theta)=\frac{1}{d}\int_0^d \sigma_{\theta\theta}(r,\theta)\mathrm{d}r=\frac{H_1}{\sqrt{2\pi}}\frac{d^{-p_1}}{(1-p_1)}F_{\theta\theta 1m}+\frac{H_2}{\sqrt{2\pi}}\frac{d^{-p_2}}{(1-p_2)}F_{\theta\theta 2m} \tag{2}$$

The distance d has to be chosen with respect to the mechanism of a failure, e.g. as a function of a size of material grain. It can be related to a fracture process zone (in the case of quasi brittle materials) or it can be gained by means of approaches presented in [19] or [20]. By analogy with cracks in the homogeneous case (MTS criterion [18]) it is assumed that the crack at the bi-material notch tip is initiated in the direction θ_0 where $\overline{\sigma_{\theta\theta,m}}(\theta)$ has its maximum. Furthermore, it is assumed that the crack is initiated when $\overline{\sigma_{\theta\theta,m}}(\theta_{0,m})$ reaches its critical value $\overline{\sigma_{\theta\theta,mC}}(\theta_{0,m})$ that is ascertained for a crack in homogeneous media. When assessing a bi-material notch, even a simple discontinuity of fracture toughness can cause incongruity between the direction of the global maximum of the mean tangential stress (Eq. 2) and the direction of the fracture initiation. The maximum value of the mean tangential stress is often found in the material m with higher Young's modulus E_m. But, if the stiffer material is tougher as well, the fracture might initiate not into the tougher material, but into the other material in the direction of the local maximum or into the bi-material interface. This question has to be answered with help of a stability criterion covering the fracture mechanics properties of both materials and the interface [24]. For the case of the steel-concrete joint, Fig. 2 shows a detail of the distribution of the tangential stress $\sigma_{\theta\theta}$ near the notch tip and Fig. 3 shows the dependence of the mean value of tangential stress on the polar coordinate θ for two averaging distances d = {0.5, 1} mm. The distances were chosen correspondingly to the size of the region with a high gradient of the stresses. The direction θ = 0° corresponds to the interface between two materials (steel and concrete). From these figures it is clear that the global maximum of the mean value of tangential stress is oriented into steel ($\theta_{0,m=2}$). Nevertheless, it is difficult to imagine fracture initiation into the steel. Thus the maxima in the other material (concrete) and at the interface corresponding to the direction $\theta_{0,m=1} = \theta_{0,\text{interface}} = 0°$ have to be considered in the stability criterion as well.

The manners of potential failure initiation and propagation are shown in Fig. 4. A crack can initiate into the substrate in the direction $\theta_{0,m=2}$ (a), into the interface $\theta_{0,\text{interface}} = 0°$ (b), or parallel to the interface into the upper material layer in the direction $\theta_{0,m=1} = 0°$ (c). In the paper only conditions of fracture initiation are studied. Therefore, the stress state before fracture initiation (stress singularity exponents and GSIFs corresponding to the notch without a crack) is considered for fracture initiation into massive materials and into the interface as well. As to the competition between the crack initiation manners, the modified MTS criterion assumes crack initiation when $\overline{\sigma_{\theta\theta,m}}(\theta_{0,m})$ reaches its critical value $\overline{\sigma_{\theta\theta,mC}}(\theta_{0,m})$, which depends on the fracture toughness K_{IC} of a homogeneous material. For a crack in a homogeneous material under mode I of loading we obtain (the direction of assumed crack propagation corresponds to $\theta_0 = 0°$):

$$\overline{\sigma_{\theta\theta,mC}}(\theta_{0,m}=0)=\frac{2K_{IC,m}}{\sqrt{2\pi d}} \tag{3}$$

Then, in order to find the direction and conditions of the crack initiation, the critical value of GSIF has to be ascertained from the comparison of Eq. 3 and Eq. 2 under critical conditions. Following the assumption of the same mechanism of a rupture in both cases (crack and notch) we obtain an expression for the $H_{1C,m}$ value:

$$H_{1C,m} = \frac{2K_{IC,m}}{\frac{d^{\frac{1}{2}-p_1}}{1-p_1} F_{\theta\theta 1m}(\theta_{0,m}) + \Gamma_{21} \frac{d^{\frac{1}{2}-p_2}}{1-p_2} F_{\theta\theta 2m}(\theta_{0,m})} \tag{4}$$

where $\Gamma_{21} = \frac{H_2}{H_1} = \frac{H_{2C}}{H_{1C}}$

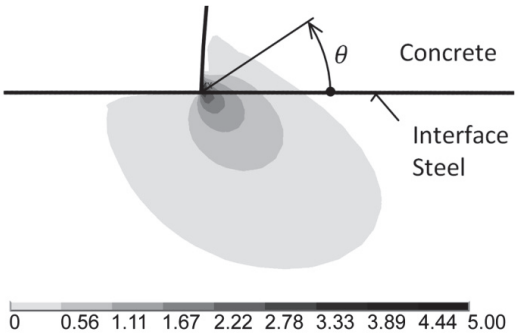

Figure 2: Distribution of the tangential stress $\sigma_{\theta\theta}$ around a rectangular bi-material notch [MPa].

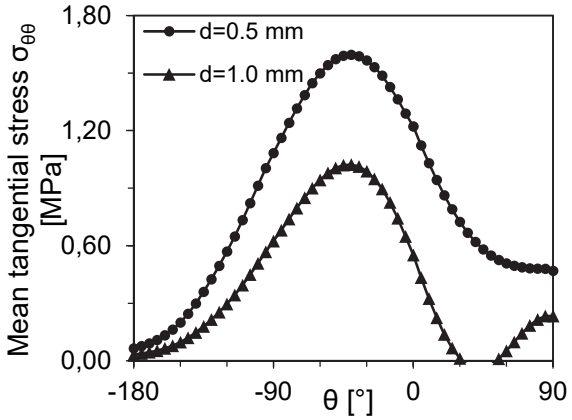

Figure 3: Distribution of the mean value of the tangential stress $\sigma_{\theta\theta}$ as a function of θ.

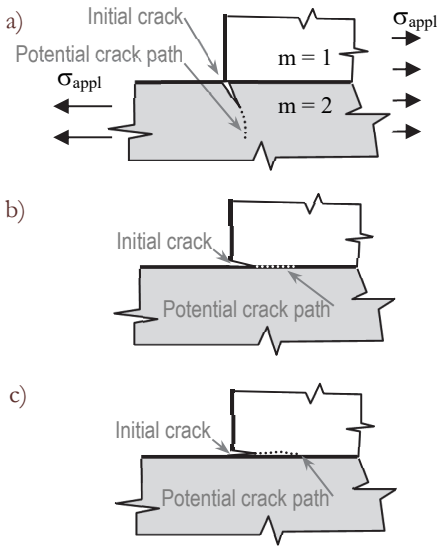

Figure 4: Possible crack initiation and failure propagation types.

The values $H_{1C,m}$ are evaluated for both materials and the interface (m = {1, 2, interface}) and they depend on the fracture toughness $K_{IC,m}$. Therefore, the critical values $H_{1C,m}$ can be called generalized fracture toughness of the notch. It may be noted that the shape functions are evaluated for the corresponding directions $\theta_{0,m}$ as well, and the direction and material of supposed fracture initiation correspond to the direction of the minimum of the values $H_{1C,1}(\theta_{0,1})$, $H_{1C,1}(\theta_{0,2})$, and $H_{1C,1}(\theta_{0,\text{interface}} = 0)$.
Finally the stability criteria can be expressed by means of GSIFs:

$$H_1 < H_{1\text{Crit}} = \min\left(H_{1C,1}(\theta_{0,1}), H_{1C,2}(\theta_{0,2}), H_{1C,\text{interface}}(\theta_0 = 0)\right) \tag{5}$$

The critical applied force can be evaluated as:

$$F_{\text{Crit}} = F_{\text{appl}} \frac{H_{1\text{Crit}}}{H_1(F_{\text{appl}})} \tag{6}$$

Fracture is not initiated in the notch tip if the GSIF (gained from a numerical solution) is lower than $H_{1\text{Crit}}$ determined as the minimum of the critical values or equivalently. This is if the applied force is lower than its critical value F_{Crit} from Eq. 6. The values of generalized fracture toughness are gained e.g. from Eq. 4.

EXPERIMENTAL OBSERVATION

Test setup

The dimensions of the push-out specimens, based on Aboobucker et al. [13], are shown in Fig. 5. In this setup a rectangular concrete block is pushed in between 2 steel plates. All samples are tested at the age of 7 days by means of push-out tests at a constant rate of 1 kN/s as shown in Fig. 6. Load spreaders with a width of 75 mm are used to convey the applied load to the concrete's top surface, generating a shear stress in the steel-concrete connection. Two dial gauges are connected to the steel plates to measure the slip between concrete and steel. In order to exclude unevenness of the test specimen, one fixed and one roller support are used. In total 28 specimens have been tested in two series.

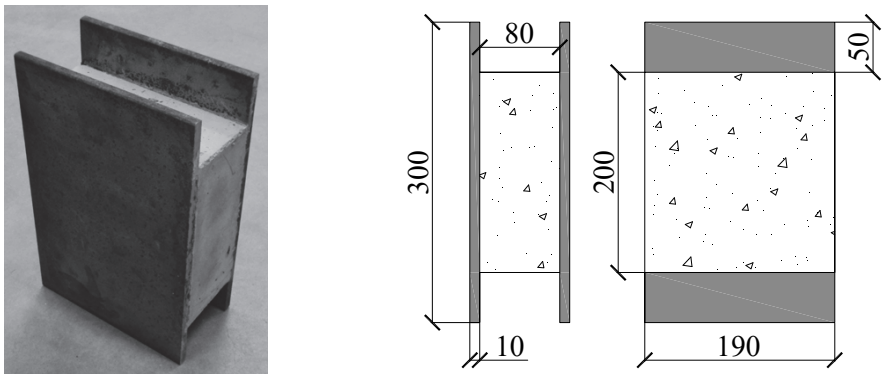

Figure 5: Dimensions of push-out test specimens [mm]

Materials

Sandblasted steel plates (S235) with a thickness of 10 mm are used. The width of these plates is chosen larger than the 6 mm in [21] or the 8 mm in [13] in order to be confident about the absence of unwanted supplementary peeling stresses caused by plate bending due to minute tolerances. They are cleaned with acetone before application of the adhesive layer to remove grease, oil, and dust, in order to achieve a better bonding performance. The following two types of adhesives used alternatively in these experiments are two-component epoxy resins. The first (rigid) adhesive is applied with a toothed paddle. Hence, this adhesive layer (epoxy 1) has vertical (as in the direction of loading) or horizontal ridges, and a minimum thickness of 2 mm with 2 mm ridges. After applying the epoxy resin mixed with hardener on the steel plates, the layer is

gritted with river gravel 2/4 or crushed stone 2/4 (Fig. 7). The second type of the adhesive is more fluid and is applied on the steel plates with a paint roller. The average thickness is only 1.5 mm. In this case, the adhesive layer is gritted with steel grit 1/2 (nominal grain size 1 to 2 mm), as seen in Fig. 8. Material properties of the epoxy interlayer are considered only for numerical calculations. For that purpose elastic constants and fracture toughness are necessary. Young's modulus E = 4750 MPa, Poisson's ratio ν = 0.39, and fracture toughness K_{IC} = 1.4 MPam$^{1/2}$.

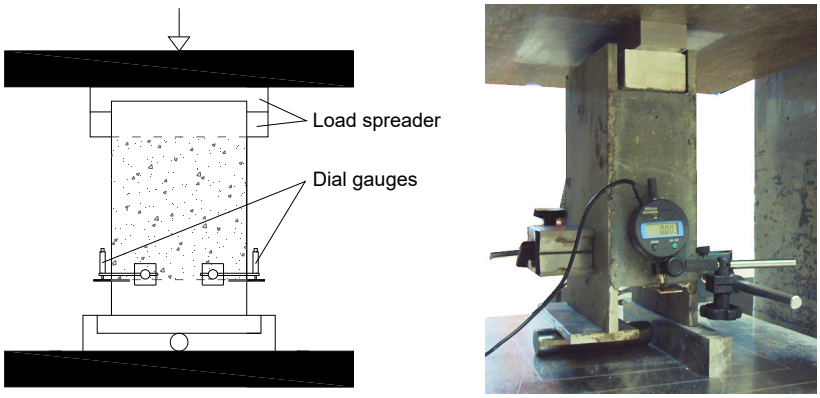

Figure 6: Test setup for push out tests

(a) (b) (c)

Figure 7: Epoxy gritting: river gravel (a), crushed stone (b), and steel grit (c).

Density [kg/m³]	f_{cm} [MPa]	f_{ctm} [MPa]	$f_{ctm,fl}$ [MPa]	E_{cm} [MPa]
2 450	130	8.5	32	38 000

Table 1: UHPC properties.

The test samples are cast with an ultra-high performance concrete (UHPC) premix REFOR-tec® GF5/ST-HS, produced by Tecnochem Italiana S.p.A. This is a tri-component cement based product (powder, liquid, and fibers), which combines the self-levelling rheology with enhanced physico-mechanical properties and ductility. Tab. 1 lists some important characteristics of this concrete according to EN 1504-3, from the technical data sheet [22]. In this table, f_{cm} is the mean value of concrete cylinder compressive strength, f_{ctm} the mean value of axial tensile strength of concrete, $f_{ctm,fl}$ the mean value of flexural tensile strength of concrete, and E_{cm} the secant modulus of elasticity of concrete.

A total of 28 specimens were cast (7 types - 4 of each type), and are listed in Tab. 2. Of these, test member 0-0-0 is prepared without an adhesive layer. Specimen 1-S-0 is made by attaching a hardened concrete prism with epoxy 1 to the steel plates under pressure in order to obtain the best adhesion between both smooth layers. Specimen 0-0-0 represents a reference for a steel concrete connection without adhesive layer, but with suitable preparation (sand blasting, cleaning). This does not correspond to an untreated connection, which according to Eurocode 1994-1-1 [23] has a shear strength of 0.6 MPa. Specimen 1-S-0 represents a reference for strengthening reinforced structures with smooth surface without concrete jetting or equivalent roughness creation. For the other specimens, the adhesive layer is applied and gritted with aggregates as described before. According to the specifications of the adhesive manufacturers, the curing time of the epoxy resins is 24

hours. After the curing of the adhesive layer, the UHPC mixture is poured into the mould, between the prepared steel plates. The test samples are demoulded after 24 hours, sealed and stored under water at 20 ± 2 °C until the age of testing at 7 days.

Name	Epoxy 1	Epoxy 2	Smooth	Ridges Hor.	Ridges Vert.	Agg A	Agg B	Agg C
0-0-0								
1-S-0	x		x					
1-R-H-a	x			x		x		
1-R-V-a	x				x	x		
1-R-H-b	x			x			x	
1-R-V-b	x				x		x	
2-S-c		x						x

Table 2: Determination of push-out specimens.

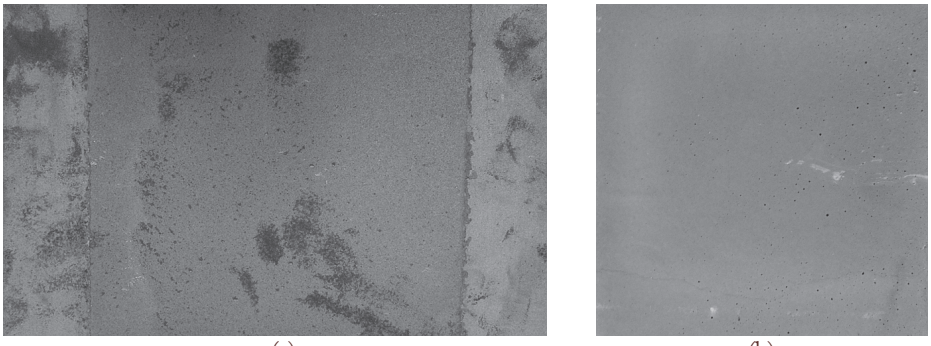

(a) (b)

Figure 8: Debonded surfaces specimen 0-0-0: steel side (a) and concrete side (b).

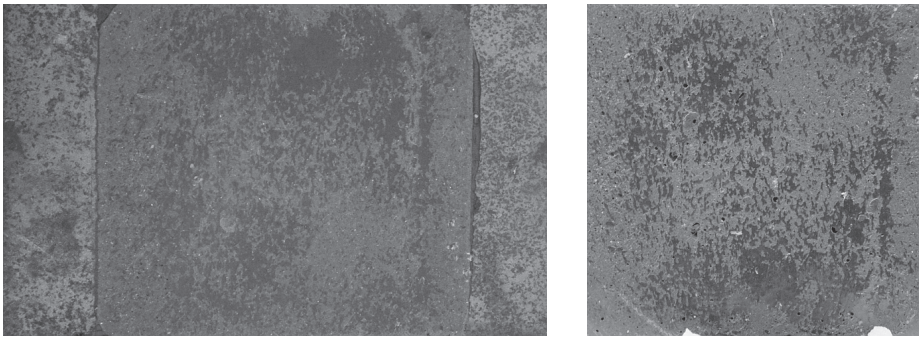

(a) (b)

Figure 9: Debonded surfaces specimen S-S-0: steel side (a) and concrete side (b).

Results and discussion

From the experimental measurement it was ascertained that all test specimens exhibited a concrete-adhesive or concrete failure. For all 1-R specimens, most of the gritted aggregates are pulled out of the adhesive layer, causing a loss of bonding between epoxy and concrete. Only for specimens 2-S-c, full concrete failure is observed. Steel and concrete surfaces after debonding can be seen in Figs. 8 to 14.

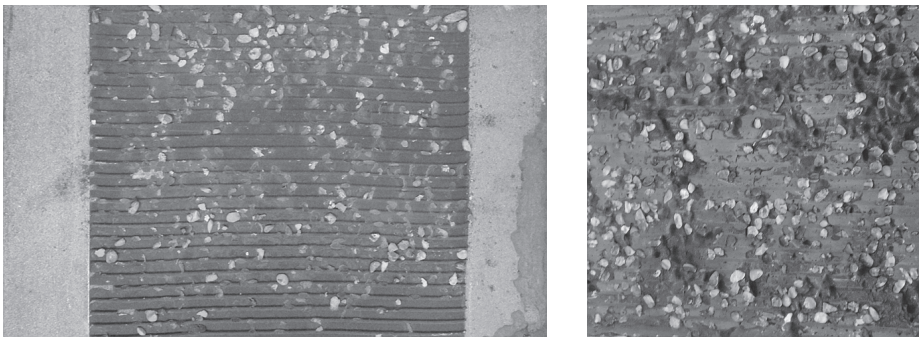

(a) (b)

Figure 10: Debonded surfaces specimen 1-R-H-a: steel side (a) and concrete side (b).

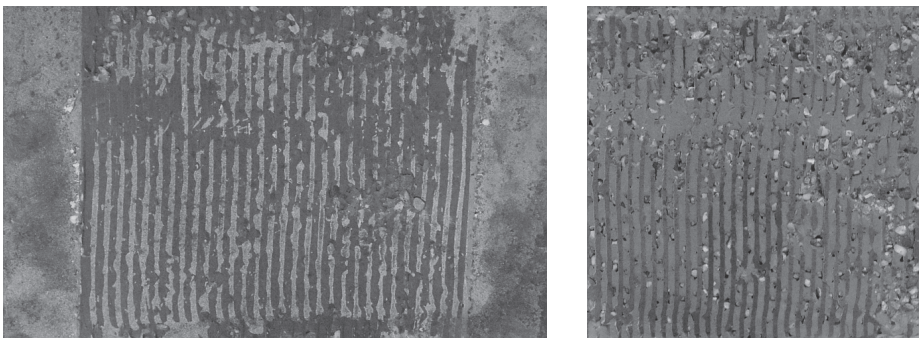

(a) (b)

Figure 11: Debonded surfaces specimen 1-R-V-a: steel side (a) and concrete side (b).

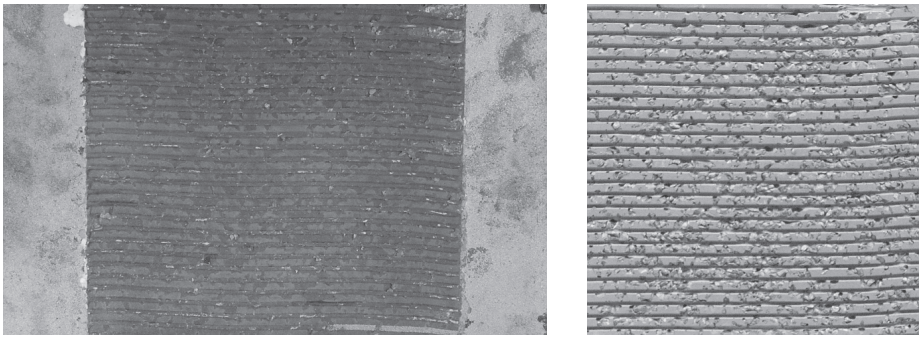

(a) (b)

Figure 12: Debonded surfaces specimen 1-R-H-b: steel side (a) and concrete side (b).

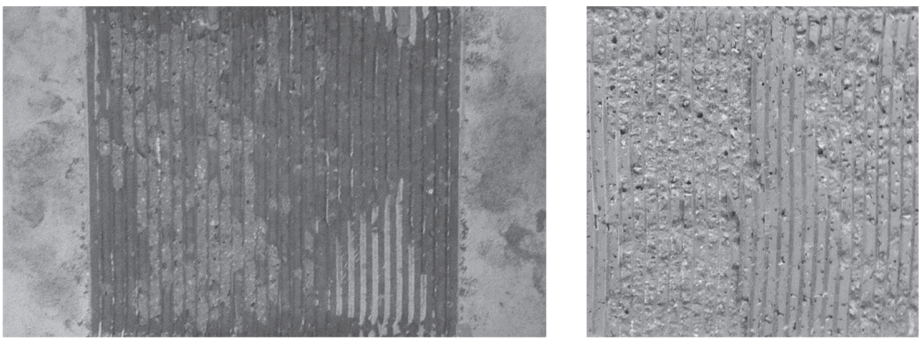

(a) (b)

Figure 13: Debonded surfaces specimen 1-R-V-b: steel side (a) and concrete side (b).

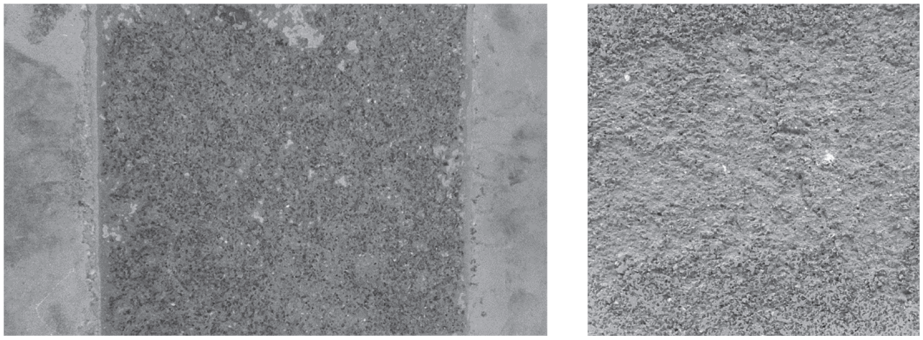

(a) (b)

Figure 14: Debonded surfaces specimen 2-S-C: steel side (a) and concrete side (b).

Test specimen	F_m [kN]	τ_m [MPa]	s_m [mm]
0-0-0	115 (21)	1.51 (0.28)	0.02 (0.01)
1-S-0	222 (45)	2.92 (0.59)	0.05 (0.03)
1-R-V-a	214 (44)	2.82 (0.57)	0.01 (0.01)
1-R-H-a	227 (29)	2.99 (0.38)	0.01 (0.01)
1-R-V-b	177 (49)	2.33 (0.64)	0.02 (0.01)
1-R-H-b	207 (53)	2.73 (0.70)	0.02 (0.02)
2-S-c	353 (85)	4.65 (1.12)	0.03 (0.01)

Table 3: Results (mean value and STDEV) of push-out tests.

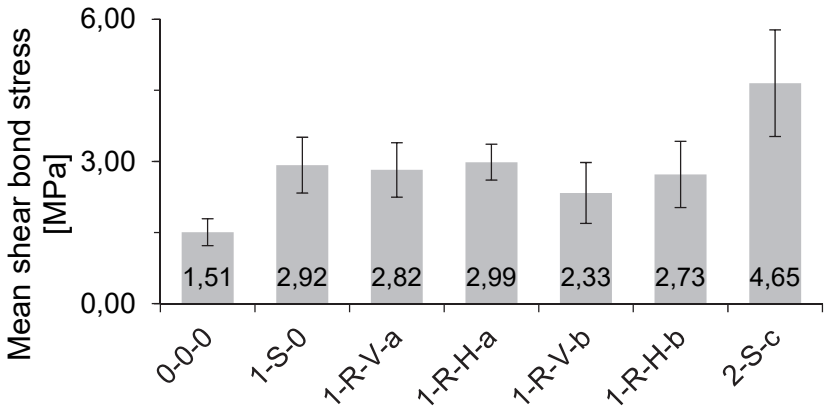

Figure 15: Results of push-out tests (graphical representation).

Tab. 3 and Fig. 15 summarize the mean values and standard deviations (STDEV) of the failure load F, the shear bond stress τ_n, and the according maximum relative slip s_m for the different push-out specimens. In this, the average shear bond stress is given by Eq. 7.

$$\tau_n = \frac{F}{A} = \frac{F}{2 \times 200 \times 190} \ [\mathrm{N/mm^2}] \tag{7}$$

From the values of Tab. 3 and Fig. 15 it can be concluded that the application of an epoxy adhesive layer improves the shear bond strength between steel plates and concrete. In addition, that test specimens 1-S-0 show a mean bond strength similar

to the samples with a gritted adhesive layer. However, it should be noted that these specimens are fabricated by gluing the steel plates on the concrete core under pressure, which improves the bond performance between steel and concrete. When push-out members with a gritted adhesive layer are mutually compared, it is clear that the experimental results for τ_n show no significant differences. It can be concluded that the use of river gravel or crushed stone as aggregates and the application of the epoxy A adhesive layer with vertical or horizontal ridges have a negligible influence on the resulting shear bond strength. Samples 2-S-C have the largest mean shear bond stress of all the tested samples. An explanation can be found in both the epoxy type, which has a higher fluidity containing less air bubbles, and the smaller gritted granules, creating a rougher adhesive layer surface. Thus the interfacial properties are improved markedly.

NUMERICAL MODELLING OF THE PUSH-OUT TEST

General characteristics of the finite element analysis model

A necessary part of the fracture mechanics assessment is numerical modelling of the test specimen. Various types of epoxy interlayer and aggregates serve as a tool for good adhesion between steel and concrete. From that point of view, a 2D model without epoxy interlayer, and 2D and 3D models with epoxy interlayer are analysed within numerical modelling. The push-out specimen is symmetrical according to its vertical axis, therefore only half of the specimen was modelled in three levels in the finite element method (FEM) software ANSYS. All the calculations serve as a part of linear elastic fracture mechanics assessments. Thus linear elastic properties of materials are considered.
First, the 2D model of the steel and concrete parts without an epoxy interlayer is performed. Second, the 2D model of the steel-epoxy-concrete connection is used. Finally, the 3D model respecting the grooved surface of the epoxy interlayer is analysed. The three models exhibit different stress concentrators in the details I and II (see Fig. 16). These details are further clarified in Fig. 17. It should be noted that the FEM models in Fig. 17 are rotated 90° anticlockwise. In the analysis, the stress concentrators in the specimen are evaluated individually.

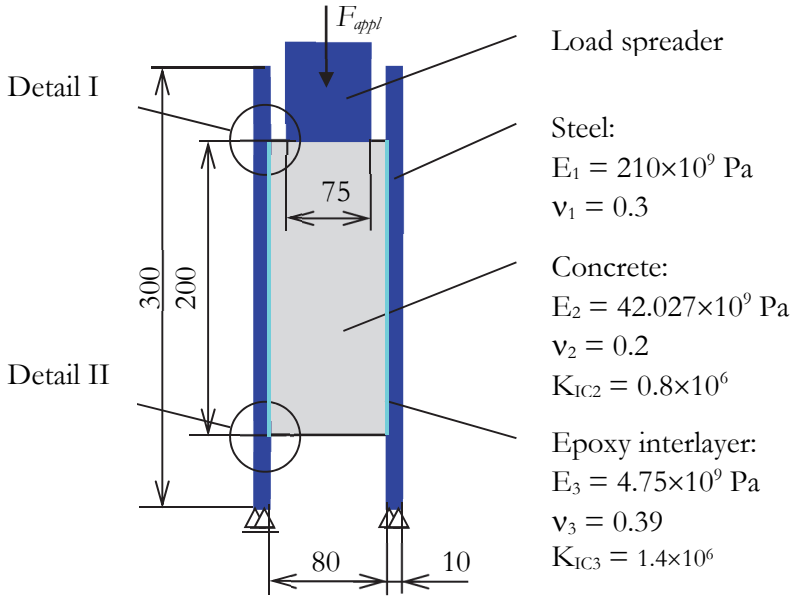

Figure 16: Geometry and material characteristics of the specimen.

2D steel-concrete FEM model

This plane-strain model is the simplest one and it contains two singular stress concentrations caused by the connection of the major material components steel and concrete. Both bi-material notches A and B (see Fig. 17a) were analysed. Due to pressure stresses near the notch B (following from the FEM analysis), the assumed crack initiation point is supposed to be the notch A. The materials and geometry of the notch imply the stress singularity exponents $p_1 = 0.3197$, $p_2 = 0.0133$ (see Eq.1, and [16, 17]). According to the MTS criterion, the global maximum of the average tangential stress is in the steel plate (Fig. 2), but because the fracture toughness K_{IC} of steel is higher than K_{IC} of concrete, the crack initiation in the direction $\theta_0 = 0°$ (the crack parallel to the interface) into concrete is supposed. The critical applied force F_{Crit} resulting from the fracture

mechanics assessment (Eq. 6) was determined in the interval <309; 343> kN, depending on the averaging distance in the criterion (See Tab. 4 for details).

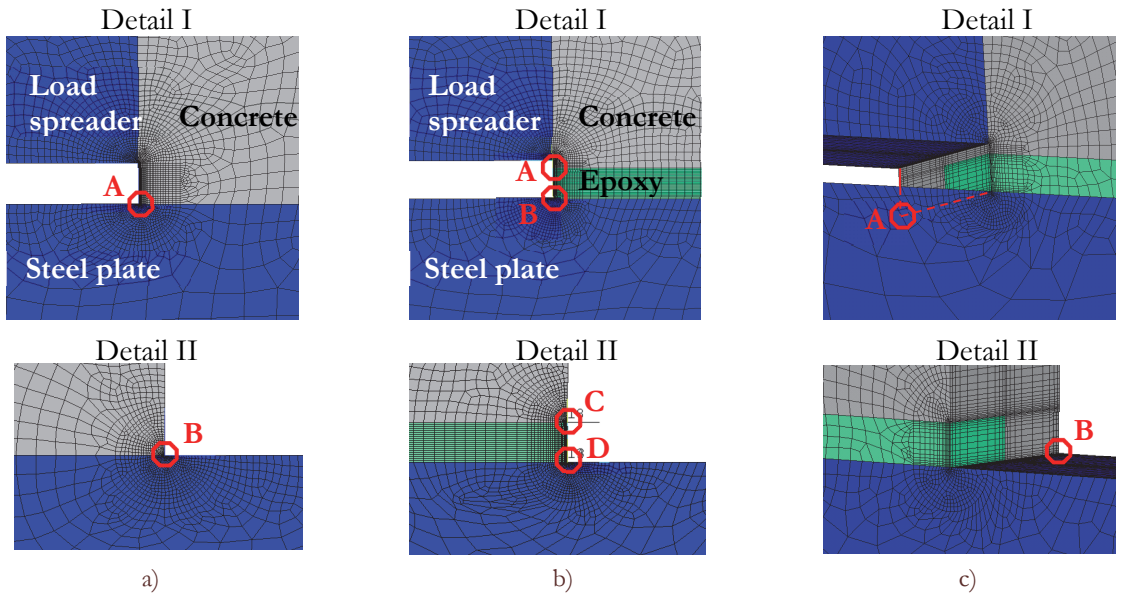

Figure 17: Geometry and material characteristics of the specimen.

		2D steel-concrete model		2D steel-epoxy-concrete model		
		Notch A	Notch A	Notch B	Notch C	Notch C
d	[mm]	0.5	1.0	0.8	0.8	0.8
θ_0	[°]	0	0	0	150	180
H_1	[Pa· m^{p1}]	1.7940×10^{5}	1.4278×10^{5}	5.2383×10^{4}	-1.3984×10^{2}	-1.3984×10^{2}
H_2	[Pa· m^{p2}]	-1.2206×10^{4}	-6.2270×10^{3}	-1.0321×10^{4}	-	-
H_{1C}	[Pa·m^{p1}]	3.8854×10^{6}	3.4342×10^{6}	4.6855×10^{6}	-2.1956×10^{4}	-3.6202×10^{2}
F_{Crit}	[kN]	308.6	342.7	1274.6	2237.2	3688.9

Table 4: Results of numerical fracture mechanics study (2D models).

2D steel-epoxy-concrete FEM model

In order to cover the presence of the epoxy interlayer, a simple 2D model of the specimen with an interlayer is suggested (see Fig. 17b). In this model four bi-material notches occur. The distribution of the average values of the tangential stress around the notches A – D is shown depending on the polar coordinate θ in Fig. 18. (θ = 0 matches to the interface). It is seen that the presence of the interlayer in the FEM model redistributes the stresses. Only in the notches B and C the stresses are positive. The negative stresses $\overline{\sigma}_{\theta\theta}$ around the notches A and D imply pressure which does not lead to failure initiation (from the supposed fracture-mechanics point of view). Therefore the notches B and C are evaluated only, and the results are stated in Tab. 4. In the case of notch B, the crack initiation angle is taken 0° as the maximum of tangential stress is in the region of the epoxy. In the case of notch C, crack initiation conditions are evaluated both in the direction of 150° (into concrete) and 180° (into epoxy). Note that in the case of notch C only one singular term occurs, thus the value H_2 is not stated. The most probable conditions for crack initiation are in notch B with F_{Crit} = 1275 kN. Nevertheless the value is considerably far from the experimental results.

3D steel-epoxy-concrete model

The results of the previously realized models lead us to survey conditions of failure initiation in the steel-concrete notch in the 3D model. The epoxy interlayer is modelled locally (see Fig. 17c) in order to represent the application of the epoxy resin

with a toothed trowel. From the analysis of the notches A and B in Fig. 17c, the resulting failure initiation forces F_{Crit} = 185902 kN are even higher than in the previous steel-epoxy-concrete 2D analysis. This unrealistic results are caused by the larger and more complicated surface of the epoxy layer, where the ideal adhesion condition are supposed in the model. The condition of ideal adhesion is the assumption of the fracture mechanics approach which is not satisfied in reality. In the case of 3D model this condition plays crucial role. Therefore the 3D model proved to be unsuitable for modelling of the push-out test specimens for the input calculation of the fracture-mechanics assessment.

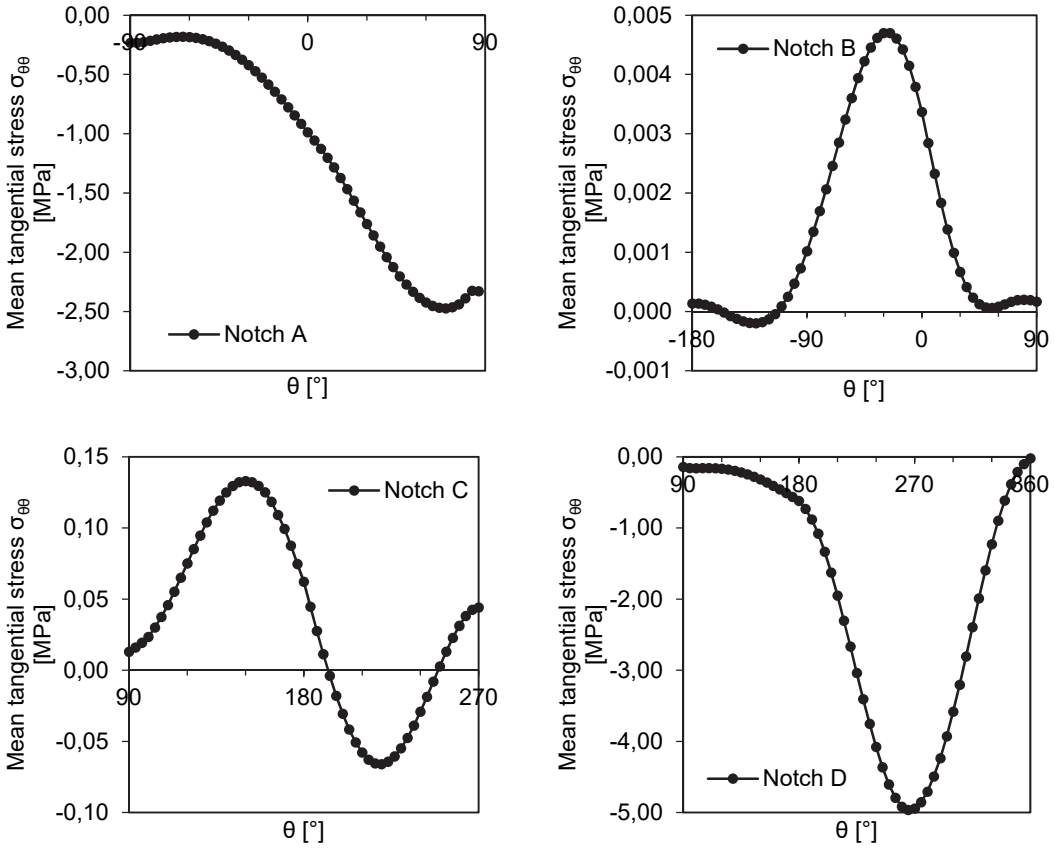

Figure 18: Average tangential stress $\overline{\sigma_{\theta\theta}}$ around notches A, B, C and D (2D steel-epoxy-concrete model).

DISCUSSION OF EXPERIMENTAL AND NUMERICAL RESULTS

Within the experimental study, the steel-concrete connections in the push-out specimens were realized in three main ways: a thick adhesive layer applied with a toothed trowel and gritted with granules, a thick smooth layer, and a thin layer of an epoxy resin with higher fluidity applied on the steel plates with a paint roller and gritted with steel grit. The fracture surface of the specimens with thick layers exhibited concrete-epoxy interfacial failure, where the F_{crit} was measured in the interval <177; 227> kN. Such cases of interfacial failure cannot be assessed by numerical-analytical approaches without knowledge of interfacial fracture toughness. On the other hand the fracture surface of the specimens with a thin layer exhibited failure in concrete and the mean value of F_{crit} = 353 kN. This corresponds well to the 2D steel-concrete model, see Fig. 17a. In this case the F_{crit} estimated by means of fracture-mechanics analysis is in the interval <309; 343> kN depending on the averaging distance in the criterion. The 2D and 3D models with thick interlayers lead to redistribution of the stresses and together with the assumption of ideal adhesion between all components these models overestimate the experimentally measured values. These models proved to be unsuitable for the purpose of modelling the push-out test samples within the input calculation of the fracture-mechanics assessment. It can be surprising that the models with the epoxy interlayer can provide less accurate results than the 2D steel-concrete model. The 2D and the 3D models with the epoxy interlayer can give more precise results in case of taking adhesion properties into account. However in this

case the fracture mechanics approach would have to be modified, the fracture mechanics properties of the steel-epoxy, steel-concrete, and epoxy-concrete interfaces would have to be measured, and the approach would lose its simplicity.
Thus the simplest 2D steel-concrete model without modelling the epoxy interlayer is the most suitable one. Due to its simplicity, it can be easily used in engineering practice.

CONCLUSIONS

Shear bond strength between steel and ultra-high performance concrete (UHPC) without mechanical shear connectors is evaluated through push-out tests and a generalized fracture mechanics approach based on analytical and finite element analyses. Based on the results of 28 test samples, the best bond behaviour is achieved with a thin rolled adhesive combined with gritted steel grit. This conclusion is important since generally for concrete to steel adhesive connections a thick epoxy is used in order to cope with tolerances. Since the concrete is cast after adhesive application, this is not an issue here. Numerical-analytical 2D and 3D modelling of a steel-concrete connection is performed without and with the epoxy interlayer. The model of a bi-material notch with various geometrical and material properties is used to simulate various singular stress concentrators that can be responsible for failure initiation. On the basis of the comparison, the 2D simulation of the steel-concrete connection without the epoxy interlayer is shown to be suitable for the estimation of failure conditions, but can only be attributed to the samples with fluid adhesive, gritted with steel grits. This connection method can therefore be considered as optimum, since from a fracture mechanics point of view it achieves the theoretical values resulting from the assumption of ideal adhesion. In this case, the weakest link is the concrete core. Higher shear load can be achieved only in combination with the use of concrete core of better fracture mechanics properties.

ACKNOWLEDGEMENTS

This research has been financially supported by the research fund of the University College Ghent and the Ministry of Education, Youth and Sports of the Czech Republic under the project CEITEC 2020 (LQ1601). The authors would like to thank the Czech Science Foundation for financial support through the Grant 16/18702S.

REFERENCES

[1] Miklofsky, H.A., Brown, M.R., Gonsior, M.J., Epoxy bonding compounds as shear connectors in composite beams. Engineering Research Series, 62–2. New York: Department of Public Works, (1962).
[2] Swamy RN, Jones R, Bloxham JW. Structural behaviour of reinforced concrete beams strengthened by epoxy-bonded steel plates. Struct Eng A, 65(2) (1987) 59–68.
[3] Barnes RA, Baglin PS, Mays GC, Subedi NK. External steel plate systems for the shear strengthening of reinforced concrete beams, Eng Struct, 23(9) (2001) 1162–1176.
[4] Yuan, H., Teng, J.G., Seracino, R., Wu, Z.S., Yao, J., Full-range behavior of FRP-to concrete bonded joints, Eng Struct, 26(5) (2004) 553–565.
[5] Lu, X.Z., Teng, J.G., Ye, L.P., Jiang, J.J., Bond-slip models for FRP sheets/plates bonded to concrete. Eng Struct, 27(6) (2005) 920–937.
[6] Ferrier, E., Quiertant, M., Benzarti, K., Hamelin P. Influence of the properties of externally bonded CFRP on the shear behavior of concrete/composite adhesive joints. Compos B: Eng 41(5) (2010) 354–362.
[7] Bouazaoui, L., Perrenot, G., Delmas, Y., Li, A., Experimental study of bonded steel concrete composite structures. J Constr Steel Res, 63 (2007) 1268–78.
[8] Thomann, M., Lebet, J.P., A mechanical model for connections by adherence for steel-concrete composite beams. Eng Struct, 30(1) (2008) 163–73.
[9] Si Larbi, A., Ferrier, E., Jurkiewiez, B., Hamelin, P., Static behaviour of steel concrete beam connected by bonding. Eng Struct, 29(6) (2007) 1034–42.
[10] Berthet, J.F., Yurtdas, I., Delmas, Y., Li, A., Evaluation of the adhesion resistance between steel and concrete by push out test, Int J Adhes Adhes, 31(2) (2011) 75–83.
[11] Zhao, G., Li, A., Numerical study of a bonded steel and concrete composite beam. Comput Struct, 86 (2008) 1830–1838.

[12] Luo, Y., Li, Z., Kang, Z., Parametric study of bonded steel–concrete composite beams by using finite element analysis, Eng Struct, 34 (2012) 40–51.
[13] Aboobucker, M.A.M., Wang, T.Y., Richard Liew, J.Y., An experimental investigation on shear bond strength between steel and fresh cast concrete using epoxy, The IES Journal A: Civil & Structural Engineering, 2(2) (2009) 107-115.
[14] Williams, M.L., The stress around a fault or crack in dissimilar media, Bull Seismol Soc Am, 49 (1959) 199-204.
[15] Klusák, J., Profant, T., Kotoul, M., Determination of the threshold values of orthotropic bi-material notches. Procedia Engineering, 2 (2010) 1635–1642.
[16] Klusák, J., Knésl, Z., Reliability assessment of a bi-material notch: Strain energy density factor approach. Theor Appl Fract Mech, 53(2) (2010) 89-93.
[17] Qian, Z.Q., Akisania, A.R., Wedge corner stress behaviour of bonded dissimilar materials, Theor Appl Fract Mech, 32 (1999) 209-222.
[18] Erdogan, F., Sih, G.C., On the crack extension in plates under plane loading and transversal shear. Int J Basic Engineering, 85(4) (1963) 519-27.
[19] Taylor, D., The theory of critical distances, Eng Fract Mech, 75 (2007) 1696-1705.
[20] Leguillon, D., Strength or toughness? A criterion for crack onset at a notch, Eur J Mech A – Solid, 21(1) (2002) 61-72.
[21] Helincks, P., De Corte, W., Klusák, J., Seitl, S., Boel, V., De Schutter, G., Failure conditions from push-out tests of a steel-concrete joint: experimental results. Key Eng Mater, 488-489 (2012) 714-717.
[22] Tecnochem Italiana S.p.A. Technical datasheet REFOR-tec GF5 ST-HS, (2010).
[23] European Committee for Standardization (CEN). EN 1994-1-1: Design of composite steel and concrete structures – Part 1-1: General rules and rules for buildings, (2004).
[24] Klusák, J., Profant, T., Knésl, Z., Kotoul, M., The influence of discontinuity and orthotropy of fracture toughness on conditions of fracture initiation in singular stress concentrators, Engineering Fracture Mechanics, 110 (2013) 438–447.